Available online at www.sciencedirect.com
ScienceDirect
Journal of Magnetic Resonance 191 (2008) 112–119
JMR Journal of Magnetic Resonance
www.elsevier.com/locate/jmr

Ingested and biomineralized magnetic material in the prey *Neocapritermes opacus* termite: FMR characterization

J.F. de Oliveira [a], O.C. Alves [b], D.M.S. Esquivel [a], E. Wajnberg [a,*]

[a] *Coordenação de Física Aplicada Departamento, Centro Brasileiro de Pesquisas Físicas, R. Xavier Sigaud, 150, Rio de Janeiro 22290-180, Brazil*
[b] *Departamento de Físico-Química da Universidade Federal Fluminense, Niterói 24020-150, Brazil*

Received 25 July 2007; revised 18 October 2007
Available online 23 December 2007

Abstract

The temperature dependence of Ferromagnetic Resonance spectra, from 5 K to 280 K, was used to study the magnetic material present in *Neocapritermes opacus* termite, the only prey of the *Pachycondyla marginata* ant. The analysis of the resonant field and peak-to-peak linewidth allowed estimating the particle diameters and the effective anisotropy energy density, K_{EFF}, as a sum of the bulk and surface contributions. It allowed to magnetically distinguish the particles of termites as collected in field from those of termites after 3 days under a cellulose diet, introduced to eliminate ingested/digested material. The data also, suggest the presence of oriented magnetite nanoparticles with diameters of 11.6 ± 0.3 nm in termites as collected in field and (14.0 ± 0.4 nm) in that under a cellulose diet. Differences between their K_{EFF} and its components are also observed. Two transitions are revealed in the resonant field temperature dependence, one at about 50 K that was associated to surface effects and the other at about 100 K attributed to the Verwey transition.

Keywords: Termite; Cellulose diet; Magnetic nanoparticles; Ferromagnetic Resonance

1. Introduction

The influence of the geomagnetic field on the behavior of animals has been studied for a long time through natural phenomena such as migration, homing, etc. Studies on several species of animals, including social insects, have shown behavioral changes during orientation and navigation, as response to the geomagnetic field [1–3]. The geomagnetic field affects the nests building and the seeking for food in different termite species [1]. The *Neocapritermes opacus* is the only alive prey of the *Pachycondyla marginata* ant, which presents a migratory behavior changing their place nests in irregular intervals of time [4]. This ant migration is significantly oriented and it is probably based on the geomagnetic field information [5] as magnetic material was found in different body parts [6]. A magnetic particle as a sensor is one of the most accepted hypothesis for magnetoreception, known as the ferromagnetic hypothesis. Although the effect of the geomagnetic field in the behavior of the *N. opacus* termite has not been shown yet, the presence of magnetic material in this prey-predator system can be related to evolutionary aspects [7].

Ferromagnetic Resonance (FMR) is a useful technique to characterize magnetic material because of the resonance spectra sensitivity to the magnetic structure size and shape. Although theoretical analysis are poorly developed to describe all aspects of experimental results, the particle shape, the diameter and the effective anisotropy constant can be estimated from the temperature dependence analysis [8–11].

Comparative FMR and SQUID magnetization measurements have shown that *N. opacus* termite contains much more magnetic material than *P. marginata* ant [7]. FMR data indicated that at least 97% of the magnetic material is in the termite body [8]. However, these results were obtained with the termite as collected in field, proba-

* Corresponding author. Fax: +55 21 21417160.
E-mail address: elianew@cbpf.br (E. Wajnberg).

1090-7807/$ - see front matter © 2007 Elsevier Inc. All rights reserved.
doi:10.1016/j.jmr.2007.12.006

bly containing biomineralized and ingested magnetic material. Ingested material is not expected to be related to magnetic orientation as its properties would not be reproducible. To achieve this functional purpose, particles must be biomineralized, to assess the required magnetic properties by physiological control. A decrease of the absorption area of FMR spectra and of the saturation magnetization, of *N. opacus* submitted to a cellulose diet was observed, at 300 K, reflecting the elimination of $35 \pm 5\%$ of magnetic material. This diet cleans their guts of ingested detrital material, reducing the contribution of non-biogenic, soil-derived magnetic particles from the analyses. Both techniques showed an apparent asymptotic behavior of those magnetic parameters in the 1–3 day diet period. Nevertheless, only the room temperature hysteresis parameters, H_c (coercive field) and J_r/J_s (remanent to saturation magnetization ratio) were shown to be independent of the diet condition, within the experimental error [12].

In the present paper, FMR temperature dependence was complementarily used to refine the results, aiming to distinguish the magnetic material size and anisotropy constant in termites as collected in field from those submitted to 3 days of iron depleted diet.

2. Materials and methods

Neocapritermes opacus workers were collected in Campinas, São Paulo, Brazil. Some of them were immediately immersed in 2.5% glutaraldehyde solution (day 0 sample) and the others fed with cellulose (paper filter) until death, which took from 1 to 4 days (day 1 to day 4 samples). No termite survives after this period. They were kept in glutaraldehyde 2.5% for 1 week and then washed three times with glutaraldehyde 2.5% in cacodylate buffer 0.1 M pH 7.4. The termites (day 0 and 3 samples) were dried for 20 min just before measurement and transferred to the Electron Paramagnetic Resonance (EPR) tubes. Termites were fixed with vacuum grease and oriented with the long body axis perpendicular to the magnetic field.

Spectra were obtained with a commercial X-band ($\nu = 9.4$ GHz) EPR spectrometer (Bruker ESP 300E) operating at a microwave power of 4 mW with a 100 kHz modulation frequency, 2×10^4 receiver gain and a modulation field of about 2 Oe in amplitude. A helium flux cryostat (Air products LTD-3-110) was used to control the temperature measured with an Au–Fe × chromel thermocouple just below the samples. The spectra temperature dependence was performed after zero field cooling (ZFC) and field cooling (FC) under 3 kOe magnetic field.

The resonant field, H_r, the field position where the spectral intensity is null, its respective effective g_{ef} factor ($g_{ef} = h\nu/\beta H_r$) and the peak-to-peak linewidth, ΔH_{pp}, were obtained directly from the spectra. The spectra intensity, SI, obtained by double integration of the experimental derivative of the absorption spectra, was calculated using the WINEPR software (Bruker). The asymmetry ratio, $A_W = \Delta H_{LF}/\Delta H_{HF}$ were calculated, where ΔH_{LF} and ΔH_{HF} are the field difference between the positions of half maximum intensities, $y_{max}/2$, in low- and high-field in the absorption spectra, obtained with WINEPR software.

3. FMR models and nanoparticles

As far as we know, there are few models to analyze nanoparticles FMR spectra, in particular, the temperature dependence [13–16], however they are limited to conditions that can not be applied to biological magnetic nanoparticle systems. Even so, they allow estimating parameters in restricted temperature ranges.

A linear temperature dependence of H_r, at temperatures higher than 100 K, is usually observed for superparamagnetic nanoparticles [13,17–19]. It was proposed for synthetic magnetite isolated nanoparticles that H_r is given by $H_r = \omega_r/\gamma - H_A$ [14,15], where $H_A = 2K_{EFF}/M_s$ is the anisotropy field of spherical nanoparticles, M_s is the saturation magnetization and $K_{EFF} = K_B + K_S$ is the effective anisotropy energy density composed by the bulk (K_B) and surface (K_S) components. The surface component relates to the surface-to-volume ratio $K_S = (6/D)k_s$, where D is the nanoparticle diameter and k_s is the surface anisotropy constant. M_s is temperature dependent, however, considering magnetite as the constituent, M_s can be taken as approximately flat (470 Oe) for temperatures far below the Curie point (850 K). Therefore, the temperature dependence of the anisotropy field follows mainly the temperature dependence of the effective surface magnetic anisotropy which was empirically associated to $(6/D)k_s = k_{eff} * T$ where k_{eff} is a size-dependent coefficient, expressed in units of erg/K cm^3. From the linear fit of $H_r(T)$ we can obtain the intercept constant A and the slope B [14,15]:

$$A = (\omega_r/\gamma - 2K_B/M_s) \tag{1a}$$

$$B = -2k_{eff}/M_s \tag{1b}$$

The H_r shift with temperature has also been interpreted considering the induced magnetization of the particle core and its surrounding amorphous region. H_r was related to the χ_m, the susceptibility of fast relaxing magnetization of the boundary region, which should obey the Curie–Weiss law, by Eq. (2):

$$\chi_m^{-1}\alpha\lambda H_r(T)/(H_0 - H_r(T))\alpha(T - \theta_C)/C \tag{2}$$

where λ is the magnetization interaction constant, θ_C the Curie temperature of the amorphous boundary and H_0 is the high temperature saturation value of H_r [20].

It was observed that for temperatures higher than 100 K, the temperature dependence of ΔH_{pp} follows the relation given by

$$\Delta H_{pp} = \Delta H_0 \tanh(\Delta E/2kT) \tag{3}$$

where $\Delta H_0 = 5g\beta Sn/d^3$ and $\Delta E = K_{EFF}V$ is associated to the magnetic energy barrier height, K_{EFF} is given by $K_{EFF} = K_B + k_{eff} * T$ and V is the particle volume. The ΔH_0 prefactor, which is the ΔH_{pp} low temperature limit, in-

cludes the Bohr magneton, β, the spin associated to the magnetic nanoparticle center, S, the number of magnetic centers in the particle, n, and the particle–particle distance, d [21].

4. Results

Examples of *N. opacus* spectra of the day 0 and day 3 ZFC samples are shown in Fig. 1. The spectra are composed of a broad line ($\Delta H_{pp} > 1000$ Oe) in the region of $g = 2$, called HF, previously associated to isolated nanoparticles [8]. The signal intensity decreases and the linewidth increases as temperature decreases. The FMR spectra at low temperatures present a line at $g = 4.3$ associated to magnetically isolated high spin ($S = 5/2$) Fe^{3+} ions in a low symmetry environment. A Mn six lines structure centered at $g = 2.01$ is easily observed at 10 K. Both Fe and Mn signal intensities strongly decrease with increasing temperatures and they are not observed at high temperatures.

Only the FC day 0 sample spectrum presents a unique line with the maximum at $g = 3.1$ clearly observed at 10 K (Fig. 1). This spectral feature has not been previously observed in the spectra of other social insects. It shifts to high field values as temperature increases and it is not resolved at temperatures above 50 K.

The g_{ef} values obtained for each spectrum are in the range from 2.10 to 2.32. The $A_W = \Delta H_{LF}/\Delta H_{HF}$ are 1.15 ± 0.05, except for day 0 sample spectra, at 5 K and 10 K, which A_W is less than 1. This reduction is due to the contribution of the $g = 3.1$ component resolved at these temperatures.

The temperature dependence of the H_r reveals two linear regions with a slope change in the 100–120 K range for day 0 sample and in the 70–100 K range for day 3 sample (Fig. 2). A shoulder is observed in the curve of the day 0 sample around 100 K that is not clear in the day 3 sample curve. At lower temperatures the decrease of H_r with the temperature is more accentuated independent of the cooling condition. A minimum is observed at a temperature that depends on the sample. For both samples, the increase of H_r at temperatures lower than that of the minimum is less intense in the FC than ZFC condition. The weak effect of field cooling is reflected on this minimum that occurs around 40 ± 10 K for day 0 sample, independent of the cooling condition. In day 3 sample curves it is observed at about 30 K under the ZFC but it is not present under the FC condition, which H_r is nearly constant below 10 K. This behavior is similar to that obtained for *P. marginata* abdomens [10] and in particular, the FC day 3 sample curve presents the same behavior as observed for the *N. opacus* body without diet [8].

The parameters A (Eq. (1a)) and B (Eq. (1b)) obtained by the linear regression of the curves in Fig. 2, for both temperature ranges are given in Table 1. In the high temperature range, the parameter A is larger in the day 3 samples than in the day 0 samples while for the low temperature range the A values are the same, within the experimental error. Taking $g = 2.12$, for magnetite at

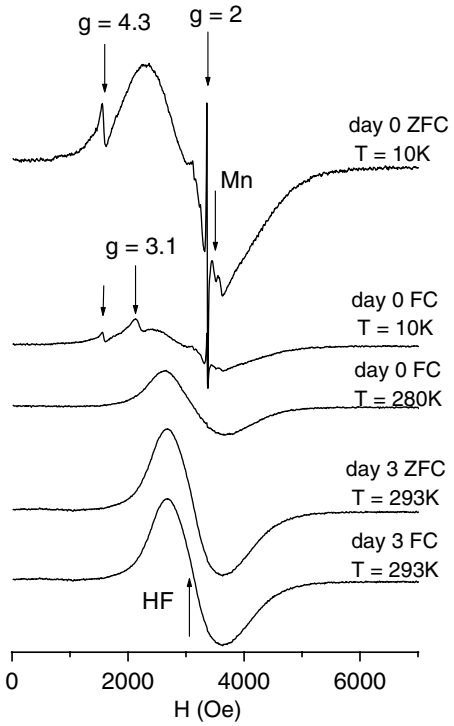

Fig. 1. FMR spectra of day 0 and day 3 samples, under 3000 Oe field cooling (FC) and zero field cooling (ZFC) conditions.

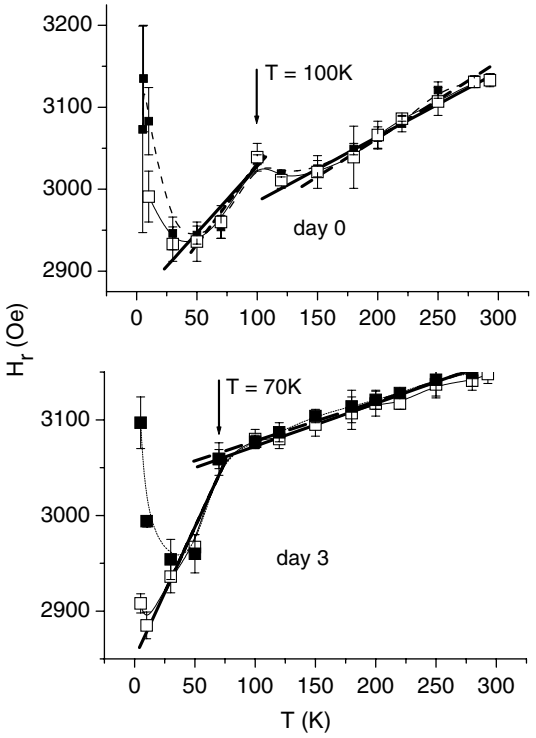

Fig. 2. Temperature dependence of the resonance field (H_r) showing the two fitted linear regions. FC (□, solid line) and ZFC (■, dashed line) conditions.

Table 1
Fitting parameters of the H_r linear temperature dependence and bulk anisotropy constant (see text for definitions)

Sample	Fitting temperature range (K)	$A = \omega_r/\gamma - 2K_B/M_s$ (Oe)	$B = -2k_{eff}/M_s$ (Oe/K)	K_B (erg/cm^3)
Day 0 ZFC	50–100	2834 ± 32	2.0 ± 0.4	$(7.8 \pm 0.8) \times 10^4$
	150–280	2875 ± 11	0.94 ± 0.05	$(6.9 \pm 0.3) \times 10^4$
Day 0 FC	30–100	2865 ± 14	1.6 ± 0.2	$(7.1 \pm 0.3) \times 10^4$
	120–280	2906 ± 7	0.79 ± 0.03	$(6.2 \pm 0.2) \times 10^4$
Day 3 ZFC	30–70	2851 ± 63	3 ± 1	$(7 \pm 2) \times 10^4$
	70–280	3036 ± 6	0.41 ± 0.03	$(3.1 \pm 0.1) \times 10^4$
Day 3FC	10–70	2851 ± 19	2.7 ± 0.4	$(7.4 \pm 0.5) \times 10^4$
	70–280	3028 ± 3	0.45 ± 0.02	$(3.29 \pm 0.07) \times 10^4$

300 K, $M_S = 470$ Oe and $\nu = 9.44001$ GHz, K_B is calculated and given in Table 1. The K_B values for the low temperature range are almost the same for all conditions, about 7×10^4 erg/cm^3, as well as for the day 0 sample at high temperature range, while for the day 3 sample the value decreases to 3.2×10^4 erg/cm^3. In the high temperature range the parameter B, which is inversely proportional to the diameter, varies from 0.41 to 0.94 and from 1.6 to 3 in the low temperature range. It is independent of the field cooling condition for day 3 sample. B values of day 0 sample are higher than day 3 sample at high temperatures and the opposite in the low temperature range.

Around 300 K the day 0 sample K_S surface contribution are $(-6.6 \pm 0.3) \times 10^4$ erg/cm^3 and $(-5.6 \pm 0.2) \times 10^4$ erg/cm^3 for ZFC and FC conditions, respectively, while the day 3 sample value is about half of the day 0 sample K_S $(-3.0 \pm 0.2) \times 10^4$ erg/cm^3. Magnetic diameters (D) are interpolated, as (11.8 ± 0.2) nm and (13.5 ± 0.2) nm for day 0 and day 3 samples, respectively, considering the linear relation between the B coefficient and $1/D$ from the magnetite nanoparticles data [14,15]. The surface anisotropy density, $k_S = 6K_S/D$, is then estimated as 1.2×10^{-2} erg/cm^2 and 0.6×10^{-2} erg/cm^2 for day 0 and day 3 samples, respectively. Only the day 3 FC sample shows a H_r saturation tendency for $T \geqslant 250$ K. The H_r values at high temperatures of each sample (Fig. 3) were then used to obtain the $\chi_m^{-1}(T)$ behavior given by Eq. (2). A linear decrease of χ_m^{-1} with decreasing temperature can be considered for $T \geqslant 200$ K, with θ_C in the 185 K to 210 K and 155 K to 185 K for the day 0 and day 3 samples, respectively.

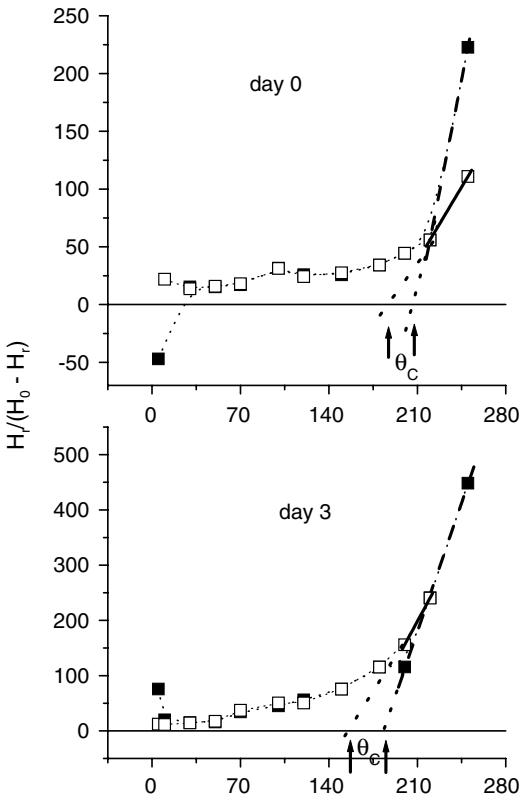

Fig. 3. $\chi^{-1} \propto H_r/(H_0 - H_r)$ temperature dependence. θ_C is the Curie–Weiss temperature of the boundary amorphous region (see text). FC (□, solid line) and ZFC (■, dashed line) conditions. The dotted curves are guide for the eyes.

By the other hand, the area under the absorption curve, SI, is proportional to the total susceptibility, χ. The normalized SI temperature dependence (Fig. 4) presents a maximum in the 70–120 K range and a shoulder at 200 K. A sharp increase below 50 K is observed (insert), except for a decrease at $T = 5$ K in the day 0 ZFC sample, not plotted in Fig. 4 to evidence the other curve features. The change of the SI and a large shift of H_r in the 70 K to 120 K range are confirmed by spectra superimposition, clearly seen in the day 3 sample data (Fig. 5). The two low temperature transitions, about 50 K and 100 K, correlate to those observed in the $H_r(T)$ curves, while the shoulder at higher temperatures could be associated to blocking temperatures, as usually observed in $\chi(T)$ by magnetometry.

The resonance linewidth (ΔH_{pp}) temperature dependence is not affected by the cooling condition within the experimental error (Fig. 6). The experimental data at the high temperature range, at least $T \geqslant 100$ K, were fitted with equation [3], because only the data in this temperature range obey this equation. Taking K_B and k_{eff} values of the high temperature range in Table 1, the fitted V values yield magnetic diameters of 11.4 ± 0.4 nm (day 0 sample) and 14.6 ± 0.6 nm (day 3 sample). The best-fit parameters obtained for ΔH_0 are (1270 ± 20) Oe and (1135 ± 20) Oe for day 0 and day 3 samples, respectively.

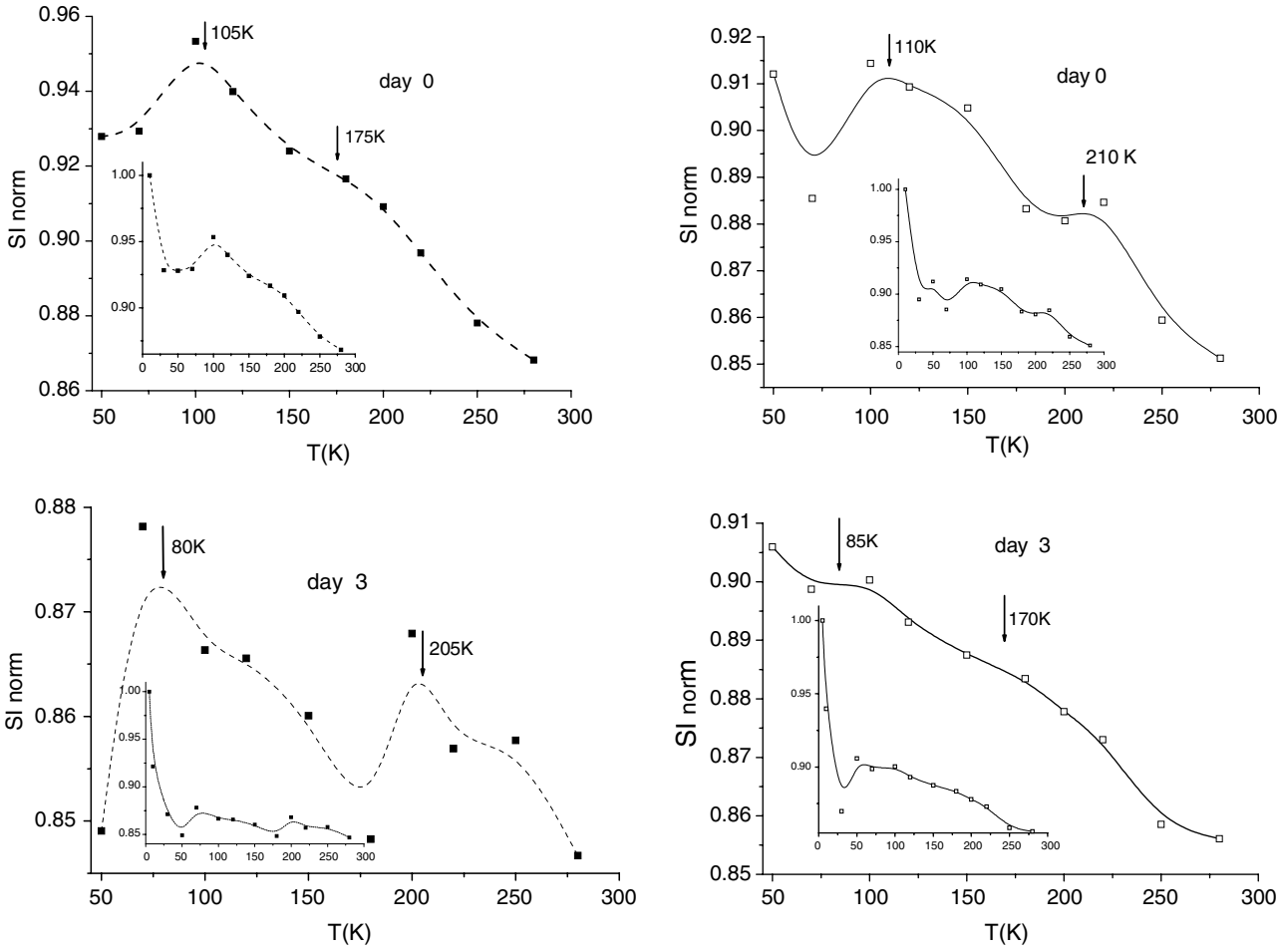

Fig. 4. Temperature dependence of FMR spectra normalized absorption area, SI. FC (□, solid line) and ZFC (■, dashed line). Inserts show $T = 5$–280 K range. Lines are guide to the eyes.

5. Discussion

The consistent decrease of the absorption area, SI, and the saturation magnetization, J_s have shown that *N. opacus* termite eliminates magnetic material when submitted to a cellulose diet, with an apparent stability after the third day [12]. Based on this result, only day 0 and day 3 samples were considered for the present analysis. Electron microscopy and magnetometry studies of other termite species have also used specimens after 3 days of cellulose diet [22]. The spectra present only a high field (HF) component, as previously observed [8,12], in contrast with other social insects that show two spectral components [9–11]. The line at $g = 3.1$ was not previously observed in other insect samples preserved in ethanol 80%, which can be associated to a material or structure that is not preserved with ethanol and/or it is eliminated by the iron depleted diet. Nevertheless, differences among individuals, nests and collects at different seasons could be responsible for the observed unexpected behavior or spectral changes mainly associated to the termite function in the nest.

The Curie–Weiss temperature ranges of the particle surface in the day 0 and day 3 termites are in good agreement with the 180 K value obtained for 4–5.5 nm superparamagnetic magnetite particles [20]. The g values extrapolated for high temperatures are between 2.13 and 2.15, in good agreement with the 2.12 magnetite value. The asymmetry ratio (A_W–1) indicates the presence of superparamagnetic magnetite nanoparticles [23]. These results support the hypothesis of magnetite nanoparticles as the main magnetic particle constituent in the *N. opacus* termite.

The H_r temperature dependences are characterized by two linear regions (Fig. 2) with a marked decrease below 100–120 K and 70–100 K for day 0 and 3 samples, respectively, and a minimum at lower temperatures (30–50 K). This behavior was observed for other magnetic nanoparticles systems. γ-Fe_2O_3 nanoparticles with a bimodal distribution of sizes below 10 nm, embedded in a polymer presented a H_r crossover temperature at about 40 K [24], while for 4 nm diameter particles, it was observed at 120 K [25], in good agreement with the observed lower crossover temperature of the sample 3 particles with larger diameter than those of sample 0. It was shown that the presence of a minimum at low temperatures (20 K) depends on the degree of dispersion of the sample [25]. Magnetite particles forming a binary system with carbide (Fe_3C) at

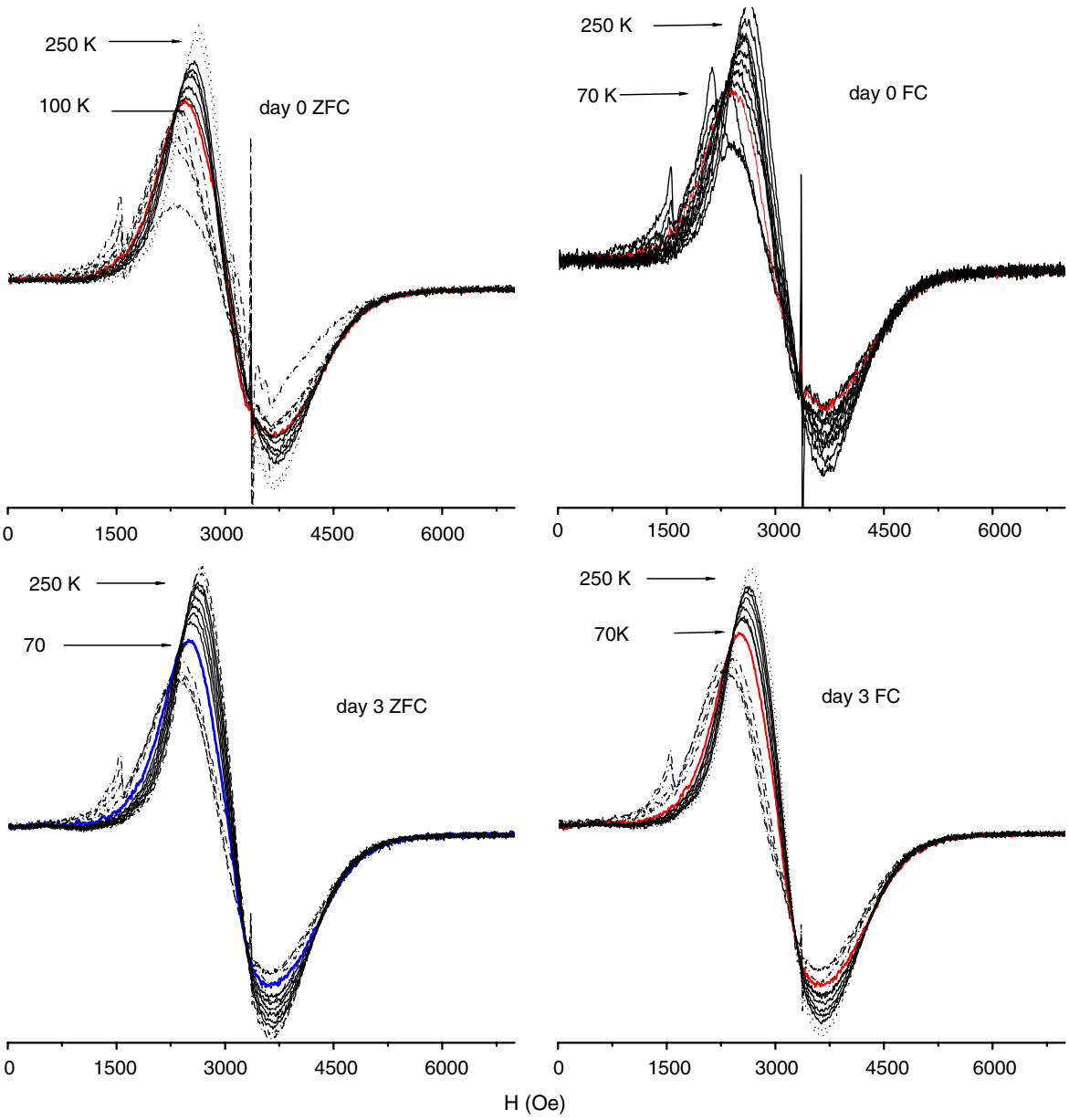

Fig. 5. Superimposed spectra. Arrows indicated the temperature transition related to H_r shift and spectra change.

low concentrations of 0.1% and 0.3% in a polymer showed an abrupt H_r change at about 115 K and 105 K and a minimum at 75.5 K and 50 K, respectively, suggesting that particles concentration in the day 3 is slightly higher than in day 0 sample [26,27]. The lower temperature transition (~50 K) has been proposed to be associated to the existence of a ferrimagnetic core surrounded by a surface layer of canted spins undergoing a spin-glass-like transition to a frozen state at this temperature. It was correlated to the sudden increase of the magnetization in the FC curves at the same temperature of to the crossover H_r temperature of maghemite nanoparticles [24,25]. A magnetization increase is clearly revealed at about 54 K in FC curves of this termite specie (unpublished data). Although the crossover of the two linear regions of $H_r(T)$ are above 54 K the minimum in the curves and the ZFC/FC magnetization curves suggest a surface effect expressed through k_{eff}. This H_r behavior combined with linewidth broadening with decreasing temperatures has been described as typical of superparamagnetic particles. The ΔH_{pp} temperature dependence does not show the noticeably broadening with the decreasing of the temperature observed in maghemite nanoparticle systems [24,25], but the observed behavior is similar to maghemite plus FeC and magnetite nanoparticles systems [25,28].

The estimated magnetic diameter of particles in the day 0 sample is lower than 18.5 ± 0.3 nm previously reported [8]. This difference results from the average H_A value considered before in the fitting of ΔH_{pp} with Eq. (3) instead of its linear temperature dependence as in the present paper.

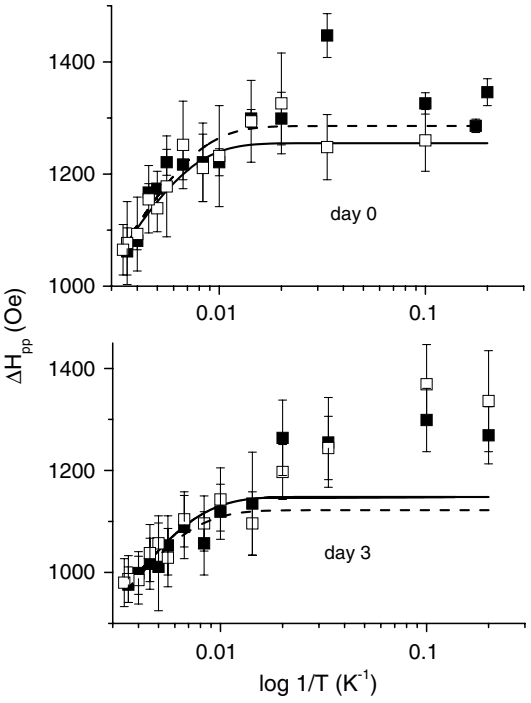

Fig. 6. Temperature dependence of the linewidth (ΔHpp), FC (□) and ZFC (■) lines are fitted with Eq. (2), FC (solid) and ZFC (dashed).

Although the present result is based on a phenomenological approach for the H_r temperature dependence; it should be a better approximation as it can be considered in the ΔH_{pp} temperature dependence. Moreover, the diameters estimated from both H_r and ΔH_{pp} are in good agreement one with each other.

It is interesting to note that the analyses of H_r data of magnetite nanoparticles were considered in the restricted temperature range from 100 K to 250 K [14,15]. In this paper the analysis was applied to the two linear regions of H_r. The high temperature range termite data yield to parameters in good agreement with those of the magnetite nanoparticles. The transition associated to the H_r slope change at about 100 K is confirmed by the SI change by spectral superimposition. A similar result was observed for 45 nm magnetite particles, which FMR signal intensity abruptly decreases at approximately 120 K as temperature decreases. It was associated to the Verwey transition [29]. The observed transition can be related to a shifted Verwey temperature, as already suggested for magnetite particle in other insects [9,11], as it is sensitive to the presence of impurities [30,31] and oxidation degree that can even suppress the transition and it affects more intensively small grains [28].

This analysis indicates the presence of nanoparticles with a positive bulk anisotropy contribution, in contrast with the well known -1.35×10^5 emu/cm^3 bulk magnetite value. The present approach results in K_s or k_s with the same order of magnitude of maghemite nanoparticles [16] and that appear as a relevant contribution to the total magnetic anisotropy. Size effects on the bulk anisotropy and anisotropy surface contribution are superparamagnetic properties frequently mentioned, but estimates values are rare or disregarded, to simplify calculations [16,17].

Considering magnetite, the differences between the materials in termites, submitted or not to diet, are revealed by the estimated K_B constant, the size-dependent coefficient, k_{eff}, and the mean particle diameter of a particle size distribution [32]. The K_B and k_{eff} values of day 3 sample are about half of those of day 0, while the estimated magnetic diameter of day 3 sample is slightly larger than the day 0 sample value, suggesting that magnetic particles of different size were eliminated by termite under the iron depleted diet. Considering that K_B should be volume independent and that only 35% of the magnetic material was eliminated by the termite under diet, the presence of other magnetic oxides, than magnetite, should be taken into account. Despite this assessment, the similarity of the termite H_r and ΔH_{pp} temperature dependences to that of synthesized nanoparticles, suggests the presence of magnetite in this insect. It is also important to bear in mind that the obtained values are estimates based on simplified models [14,15,20] on isolated nanoparticles for which interparticle interactions, for example, are disregarded.

6. Conclusions

The present temperature dependence results reveals the diet effect on the averaged estimated magnetic parameters of the particles, that was not observed by previous RT FMR and magnetometry measurements [12].

The weak effect of the cooling field, shown by the similarity of the ZFC and FC magnetic parameters (Table 1 and Figs. 2, 3 and 6), indicates a high fraction of orientated particles with the easy magnetization axis parallel to this field, that is, perpendicular to the long body axis of the termite, as previously suggested [8].

The termite magnetic particle system seems to be composed of superparamagnetic particles of ~14 nm instead of single domain particles associated to magnetotaxy in microorganism and magnetoreception in other animals [2]. Nevertheless, it has been proposed that a cluster of superparamagnetic particles could self-organize in chains that behave themselves as a compass under determined magnetic fields [33], therefore the orientation system is not limited to single domains (SD). The termite particle sizes are larger than the 1–5 nm magnetite grain sizes identified in the upper beak tissue of pigeons [34], recently demonstrated to be associated to maghemite particles in a complex structure [35]. Those particles are, however, in the range of those find in other insects [9–11], in particular, its predator, the *P. marginata* ant, stimulating the study of the evolutionary aspect in this prey-predator system. The size and orientation of the termite magnetic particles fulfill functional characteristics, as those of magnetoreceptive systems in social insects.

Acknowledgments

We thank Dr. P. S. Oliveira and H. Dutra for termite supply. E.W. thanks CNPq for financial support and J.F. de Oliveira thanks the CNPq for a fellowship.

References

[1] M. Vácha, Magnetic orientation in insects, Biologia, Bratislava 52 (1997) 629–636.
[2] R. Wiltschko, W. WiltschkoMagnetic Orientation in Animals, vol. 33, Springer, Berlin, 1995.
[3] C.Y. Hsu et al., Magnetoreception system in honeybees (*Apis mellifera*), PLoS ONE 2 (2007) e395, doi:10.1371/journal.pone.0000395.
[4] I. Leal, P.S. Oliveira, Behavioral ecology of the neotropical termite hunting ant *Pachycondyla* (=Termitopone) *marginata*—colony founding, group-raiding and migratory patterns, Behav. Ecol. Sociobiol. 37 (1995) 373–383.
[5] D. Acosta-Avalos et al., Seasonal patterns in the orientation system of the migratory ant *Pachycondyla marginata*, Naturwissenschaften 88 (2001) 343–346.
[6] E. Wajnberg, Antennae: the strongest magnetic part of the migratory ant, Biometals 17 (2004) 467–470.
[7] D.M.S. Esquivel et al., Comparative magnetic measurements of migratory ant and its only termite prey, J. Magn. Magn. Mater. 278 (2004) 117–121.
[8] O.C. Alves et al., Magnetic material arrangement in oriented termites: a magnetic resonance study, J. Magn. Reson. 168 (2004) 246–251.
[9] L.J. El-Jaick et al., Electron paramagnetic resonance study of honeybee *Apis mellifera* abdomens, Eur. Biophys. J. 29 (2001) 579–586.
[10] E. Wajnberg et al., Electron paramagnetic resonance study of the migratory ant *Pachycondyla marginata* abdomens, Biophys. J. 78 (2000) 1018–1023.
[11] L.G. Abraçado et al., thorax and abdomen of *Solenopsis substituta* ants: a ferromagnetic resonance study, J. Magn. Reson. 175 (2005) 309–316.
[12] J.F. Oliveira et al., Magnetic resonance as a technique to magnetic biosensors characterization in *Neocapritermes opacus* termites, J. Magn. Magn. Mater. 294 (2005) e171–e174.
[13] R. Berger et al., Temperature dependence of superparamagnetic resonance of iron oxide nanoparticles, J. Magn. Magn. Mater. 234 (2001) 535–544.
[14] P.C. Morais et al., Magnetic resonance of magnetite nanoparticles dispersed in mesoporous copolymer matrix, IEEE T. Magn. 36 (2000) 3038–3040.
[15] P.C. Morais et al., Magnetic resonance of magnetic fluid and magnetoliposome Preparations, J. Magn. Magn. Mater. 293 (2005) 526–531.
[16] F. Gazeau et al., Magnetic resonance of ferrite nanoparticles: evidence of surface effects, J. Magn. Magn. Mater. 186 (1998) 175–187.
[17] K. Nagata, A. Ishihara, ESR of ultra fine magnetic particles, J. Magn. Magn. Mater. 104 (1992) 1571–1573.
[18] N. Guskos et al., Matrix effects on the magnetic properties of γ-Fe_2O_3 nanoparticles dispersed in a multiblock copolymer, J. Appl. Phys. 99 (2006) 084307-1–084307-7.
[19] T. Bodziony et al., Ferromagnetic resonance study of $Fe_3O_4$and Fe_3C magnetic nanoparticle mixture filling the PTMO-block-PET polymer, Rev. Adv. Mater. Sci. 8 (2004) 86–91.
[20] M. Hagiwara, K. Nagata, Magnetic behaviors of complex nature found in an oxide glass system containing deposited magnetite clusters at the superparamagnetic state, J. Magn. Magn. Mater. 177 (1998) 91–92.
[21] P.C. Morais et al., Electron spin resonance in superparamagnetic particles dispersed in a non-magnetic matrix, Philos. Magn. Lett. 55 (1987) 181–183.
[22] B.A. Maher, Magnetite biomineralization in termites, Proc. R. Soc. Lond. B 265 (1998) 733–737.
[23] B.P. Weiss et al., Ferromagnetic resonance and low temperature magnetic tests for biogenic magnetite, Earth Planet. Sci. Lett. 224 (2004) 73–89.
[24] Y.A. Koksharov et al., Electron paramagnetic resonance near the spin-glass transition in iron oxide nanoparticles, Phys. Rev. B 63 (2000) 0124071–0124074.
[25] N. Guskos et al., Matrix effects on the magnetic properties of γ-Fe_2O_3 nanoparticles dispersed in a multiblock copolymer, J. Appl. Phys. 99 (2006) 084307-1–084307-7.
[26] T. Bodziony et al., Low Concentration effect of Fe_3O_4 and Fe_3C magnetic nanoparticles in non-magnetic matrix on the FMR spectra, Acta Phys. Pol. A 108 (2005) 297–302.
[27] T. Bodziony et al., Temperature dependence of the FMR spectra of Fe_3O_4 and Fe_3C nanoparticle magnetic systems in copolymer matrices, Mater. Sci.-Poland 23 (2005) 1056–1063.
[28] O. Ozdemir, D.J. Dunlop, B.M. Moskowitz, The effect of oxidation on the Verwey transition in magnetite, Geophys. Res. Lett. 20 (1998) 1671–1674.
[29] J. Wang et al., Disappearing of the Verwey transition in magnetite nanoparticles synthesized under a magnetic field: implications for the origin of charge ordering, Chem. Phys. Lett. 390 (2004) 55–58.
[30] B.M. Moskowitz, M. Jackson, C. Kissel, Low-temperature magnetic behavior of titanomagnetites, Earth Planet. Sci. Lett. 157 (1998) 141–149.
[31] N. Guigue-Millot, N. Keller, P. Perriat, Evidence for the Verwey transition in highly nonstoichiometric nanometric Fe-based ferrites, Phys. Rev. B 64 (2001). Art. No. 012402-1-012402-4.
[32] D. Acosta-Avalos et al., Isolation of magnetic nanoparticles from *Pachycondyla marginata* ants, J. Exp. Biol. 202 (1999) 2687–2692.
[33] A.F. Davila et al., Magnetic pulse affects a putative magnetoreceptor mechanism, Biophys. J. 89 (2005) 56–63.
[34] M. Hanzlik et al., Superparamagnetic magnetite in the upper beak tissue of homing pigeons, BioMetals 13 (2000) 325–331.
[35] G. Fleissner et al., A novel concept of Fe-mineral-based magnetoreception: histological and physicochemical data from the upper beak of homing pigeons, Naturwissenschaften 94 (2007) 631–642.